

Alpha Spectroscopy of  $^{212g}\text{At}$  and  $^{212m}\text{At}^\dagger$ 

PAUL L. REEDER

*Department of Chemistry, Washington University, St. Louis, Missouri 63130*

(Received 29 September 1969)

The  $\alpha$  decay of  $^{212g}\text{At}$  and  $^{212m}\text{At}$  to excited states of  $^{208}\text{Bi}$  has been measured. Half-lives of  $0.315 \pm 0.003$  and  $0.122 \pm 0.001$  sec were determined in agreement with previous work. Out of a possible 28 transitions, 20  $\alpha$  transitions were observed to states in  $^{208}\text{Bi}$  below 1.11-MeV excitation.

## I. INTRODUCTION

THE two isomers of  $^{212}\text{At}$  were first discovered by Jones,<sup>1</sup> who reported half-lives of 0.305 sec for  $^{212g}\text{At}$  and 0.120 sec for  $^{212m}\text{At}$ . He observed two  $\alpha$  groups from each isomer which indicated that the  $\alpha$  decay populates both the ground and first excited states of  $^{208}\text{Bi}$  with high intensity. Later work by Valli and Hyde<sup>2</sup> gave slightly revised energies for the four  $\alpha$  groups.

The  $^{208}\text{Bi}$  daughter from  $\alpha$  decay of  $^{212}\text{At}$  is of special interest because it consists of one proton more and one neutron less than the doubly magic nuclide  $^{208}\text{Pb}$ . Consequently, the excited states of  $^{208}\text{Bi}$  can be calculated quite accurately with shell-model methods.<sup>3</sup> The agreement between the calculations and experimental measurements<sup>4,5</sup> of the excited states is remarkably good. The experimental measurements were performed by  $^{207}\text{Pb}(^3\text{He}, d)^{208}\text{Bi}$  and  $^{209}\text{Bi}(d, t)^{208}\text{Bi}$  reactions. Excited states of  $^{208}\text{Bi}$  were also measured by  $\text{Ge}(\text{Li})$   $\gamma$  spectroscopy following decay of the  $^{208}\text{Bi}$  isomer at 1.57 MeV.<sup>6</sup>

The  $\alpha$  decay of  $^{212}\text{At}$  provides an additional means of observing the excited states of  $^{208}\text{Bi}$ . Since  $^{212g}\text{At}$  and  $^{212m}\text{At}$  have spins and parities of  $1^-$  and  $9^-$ , respectively,<sup>1,7</sup> the relative intensities of  $\alpha$  peaks from  $^{212g}\text{At}$  will differ from the relative intensities of peaks from  $^{212m}\text{At}$  depending on the spins of the states in  $^{208}\text{Bi}$ . For example,  $^{212g}\text{At}$  should strongly populate a  $2^+$  state in  $^{208}\text{Bi}$  by means of an  $L=1$  transition, whereas  $^{212m}\text{At}$  should not populate it owing to the strong angular momentum barrier for an  $L=7$  transition. Thus, the  $\alpha$  spectra provide information on the spins as well as the energies of the states of  $^{208}\text{Bi}$ . In addition, the determination of relative intensities for  $\alpha$  decay from  $^{212}\text{At}$  provides data for comparison with theoretical calculations of  $\alpha$ -decay rates to excited states.<sup>8</sup>

## II. EXPERIMENTAL METHODS AND RESULTS

The  $^{212}\text{At}$  was produced at the Washington University 54-in. cyclotron by means of the  $^{209}\text{Bi}(^4\text{He}, n)^{212}\text{At}$  reaction. The bombarding energy of 23 MeV was chosen to maximize the yield of the  $(^4\text{He}, n)$  reaction and to minimize the yield of the  $(^4\text{He}, 2n)$  reaction. All experiments were performed in an 18-in. scattering chamber located beyond a 4-ft-thick concrete shielding wall. Because of the short half-lives, the cyclotron beam was pulsed repetitively and  $\alpha$  spectra were accumulated between beam bursts. The beam was pulsed by means of a pulse-triggered mercury relay which interrupted the cyclotron rf power at a low-power stage. A typical target consisted of a few mg/cm<sup>2</sup> of bismuth evaporated onto a 0.0001-in. nickel foil. The bismuth faced downstream and  $^{212}\text{At}$  ions which recoiled out of the target were collected downstream on a very thin catcher foil.

## A. Half-Lives

In an experiment to measure the half-lives, a stationary catcher foil of 0.0001-in. nickel was viewed by a 3-cm<sup>2</sup>-area 300- $\mu$ -thick gold surface-barrier detector. The detector was shielded from the target by a 0.25-in. aluminum plate. Between the catcher foil and the detector was a 1200-G magnet followed by a 2.85-cm<sup>2</sup> collimator. The magnetic field eliminated fluctuations of the leakage current in the detector during beam-on-beam-off times. After amplification the detector signals passed through a biased amplifier and were stored in a 4096-channel pulse-height analyzer. The analyzer operated in a "multispectra mode" in which 512-channel energy spectra were stored for eight successive time periods of 100 msec each. A "predetermined timer" with four outputs was used to automatically control the functions of beam on, beam off, analyzer on, and analyzer off. For this experiment, one cycle consisted of 300 msec of beam on, a 10-msec delay, and then 800 msec of analyzer on. About 10 000 cycles were required to obtain enough statistics to perform decay curve analysis on the prominent  $\alpha$  peaks to the ground and first excited states of  $^{208}\text{Bi}$ . The resolution [full width at half-maximum (FWHM)] was 53 keV, which was sufficient to completely resolve the two  $^{212g}\text{At}$  peaks from the two  $^{212m}\text{At}$  peaks. However, the separation of the ground and first excited states in  $^{208}\text{Bi}$  is about 64

<sup>†</sup> Work supported by the U.S. Atomic Energy Commission.

<sup>1</sup> W. B. Jones, Phys. Rev. **130**, 2042 (1963).

<sup>2</sup> K. Valli and E. K. Hyde, Phys. Rev. **176**, 1377 (1968).

<sup>3</sup> Y. E. Kim and J. O. Rasmussen, Phys. Rev. **135**, B44 (1964).

<sup>4</sup> J. R. Erskine, Phys. Rev. **135**, B110 (1964).

<sup>5</sup> W. P. Alford, J. P. Schiffer, and J. J. Schwartz, Phys. Rev. Letters **21**, 156 (1968).

<sup>6</sup> M. Bonitz, J. Kantele, and N. J. Sigurd Hansen, Nucl. Phys. **A115**, 219 (1968).

<sup>7</sup> Y. Kim and J. O. Rasmussen, Nucl. Phys. **47**, 184 (1963).

<sup>8</sup> H. J. Mang, Ann. Rev. Nucl. Sci. **14**, 1 (1964).

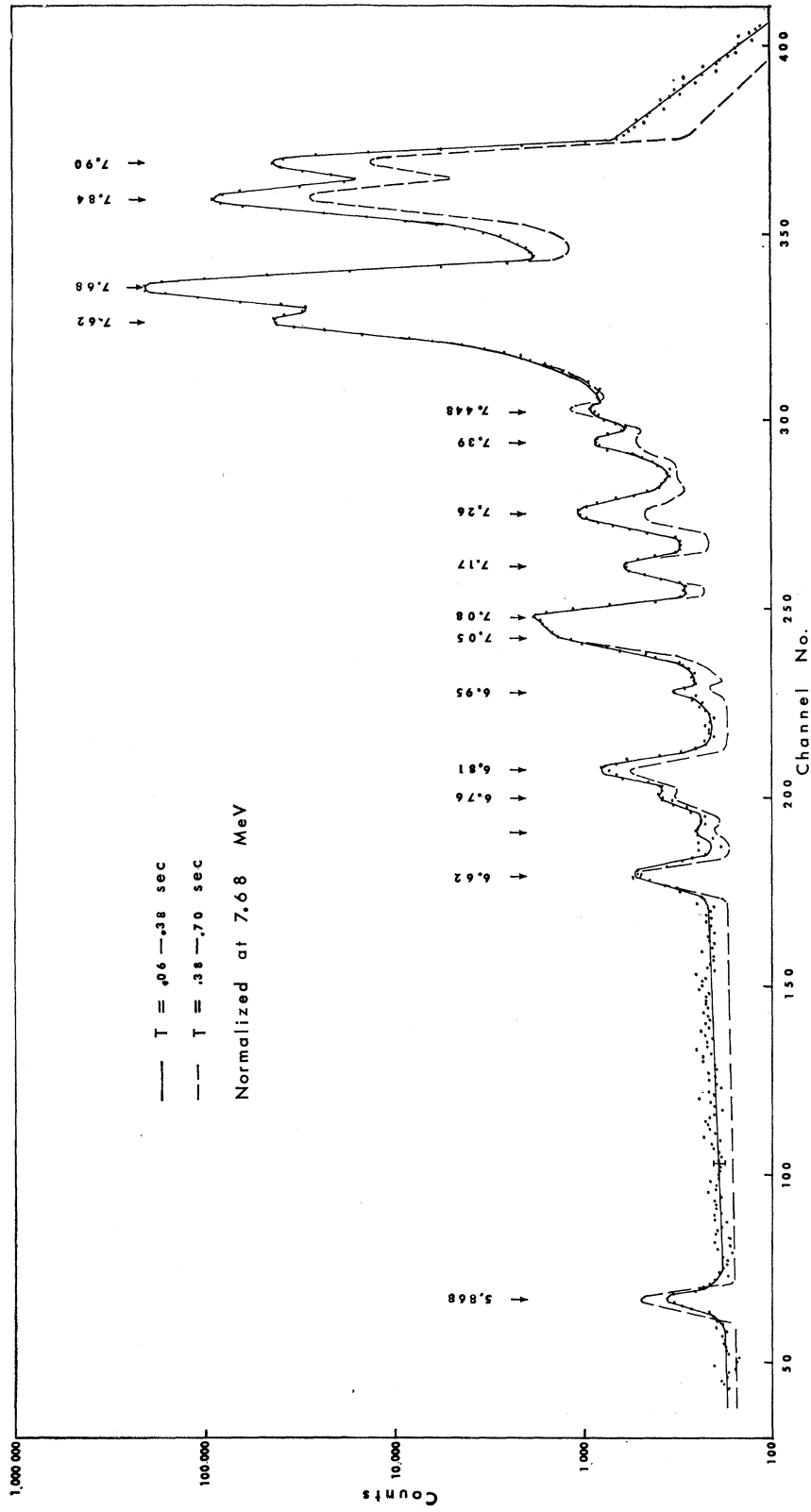


Fig. 1. Comparison of  $^{212}\text{At}$   $\alpha$  spectra at two time intervals after bombardment. Kinetic energies of  $\alpha$  particles are given above the peaks. Data points and solid line refer to early spectrum. Dashed line refers to later spectrum normalized at 7.68-MeV peak.

keV so that these two states were not well resolved from each other. The areas under the combined ground- and first-excited-state peaks were integrated for each time channel and least-squares decay-curve analysis was performed by the computer program CLSQ.<sup>9</sup> The resulting half-lives are  $0.315 \pm 0.003$  sec for  $^{212g}\text{At}$  and  $0.122 \pm 0.001$  sec for  $^{212m}\text{At}$ . These values are in excellent agreement with the previously measured half-lives.<sup>1</sup>

In order to observe  $\alpha$  transitions to the higher excited states of  $^{208}\text{Bi}$ , a system with higher resolution and higher counting efficiency was developed. The stationary catcher foil was replaced by a 6-in.-diam wheel which held nine 0.0001-in.-thick iron catcher foils spaced at 40-deg intervals around the circumference. The wheel was driven by a stepping motor which turned 40 deg in 56 msec. The target was mounted about  $\frac{1}{8}$  in. upstream from the catcher foil. After the beam burst the catcher foil was rotated 40 deg to place the catcher directly in front of a 2.0-cm<sup>2</sup>-area surface-barrier detector with a depletion depth of 300  $\mu$ . This detector gave a total resolution of about 35 keV. The detector was shielded from beam scattered from the target and the catcher foil.

This system was used to obtain spectra at two successive time intervals after bombardment in order to distinguish  $\alpha$  spectra of  $^{212m}\text{At}$  from  $^{212g}\text{At}$ . The bombardment and counting cycle consisted of 300 msec of beam, 60 msec for the wheel to turn, 320 msec of counting for spectrum one and 320 msec of counting for spectrum two. This cycle was repeated about 22 000 times to obtain the two spectra shown in Fig. 1. The data points and solid curve refer to the earlier spectrum and the

TABLE I. Half-lives for individual  $\alpha$  peaks.

$\alpha$ -particle energy (MeV)	Half-life (msec)	Assignment <sup>a</sup>
7.90	$118 \pm 6$	<i>m</i>
7.84	$119 \pm 6$	<i>m</i>
7.68	$334 \pm 17$	<i>g</i>
7.62	$308 \pm 15$	<i>g</i>
7.45	no decay	$^{211}\text{Po}$
7.39	$156 \pm 11$	<i>m</i>
7.26	$124 \pm 8$	<i>m</i>
7.17	$446 \pm 26$	<i>g</i>
7.08	$314 \pm 17$	<i>g</i>
7.05		<i>g</i>
6.95	$96 \pm 21$	<i>m</i>
6.81	$185 \pm 11$	<i>g, m</i>
6.76	$272 \pm 21$	<i>g</i>
6.62	$335 \pm 20$	<i>g</i>
5.87	no decay	$^{211}\text{At}$

<sup>a</sup> *m* =  $^{212m}\text{At}$ , *g* =  $^{212g}\text{At}$ .

<sup>9</sup> J. B. Cumming, U.S. Atomic Energy Commission Report No. NAS-NS3107, 1962, p. 25 (unpublished).

TABLE II. Experimental conditions for high-resolution spectra.

	Run A	Run B
Beam on (msec)	300	300
Delay (msec)	50	30
Analyzer on (msec)	200	300
Cycles	33 000	114 000

dashed curve refers to the later spectrum. The later spectrum has been normalized to the earlier spectrum at the most intense peak in the  $^{212g}\text{At}$  spectrum. Thus, in the later spectrum peaks with the same half-life as  $^{212g}\text{At}$  (315 msec) coincide with the solid curve, peaks with a shorter half-life ( $^{212m}\text{At}$  = 122 msec) fall below the solid curve, and peaks with a longer half-life rise above the solid curve. The areas under the peaks were integrated and half-lives for each peak were calculated based on the two time points. The half-life results and peak assignments from this experiment are listed in Table I. The errors given in Table I for the half-lives are determined by rms addition of two types of error—a constant 5% error in half-life due to uncertainty in fitting a background and integrating the area under the  $\alpha$  peaks and a variable error dependent on the counting statistics.

Both the 7.45- and 5.87-MeV peaks are due to decay of 7.21-h  $^{211}\text{At}$  produced by the ( $^4\text{He}, 2n$ ) reaction. The two peaks did not overlap any  $^{212}\text{At}$  peaks and were convenient points for energy calibration so no attempt was made to eliminate them by bombarding at a lower energy.

## B. Energy Spectra

From Fig. 1, it is apparent that some peaks are composites of several  $\alpha$  peaks and that even better resolution is needed. A small (0.25-cm<sup>2</sup>) surface-barrier detector<sup>10</sup> with system resolution of 23 keV was then used in two experiments to measure the energy spectrum only. In run A, the 6-in.-diam catcher wheel was used and in run B, a 12-in.-diam catcher wheel was used. The larger wheel had 24 catcher foils of 0.0002-in.-thick aluminum spaced at 15-deg intervals on the circumference. The transit time from the target position to the counting position was 30 msec for a 15-deg rotation of the wheel. The  $^4\text{He}$  beam was moved slightly off the center of the catcher wheel to avoid striking the catcher foil 180 deg from the target. The larger number of catcher foils is desirable to reduce the long-lived background activity produced by multiple exposures of the catcher foils to the beam. The experimental details for runs A and B are given in Table II.

The spectrum obtained in run A is shown in Fig. 2 since it shows the shorter-lived peaks to best advantage. The spectrum obtained in run B had twice the number

<sup>10</sup> This detector was kindly loaned by D. G. Sarantites.

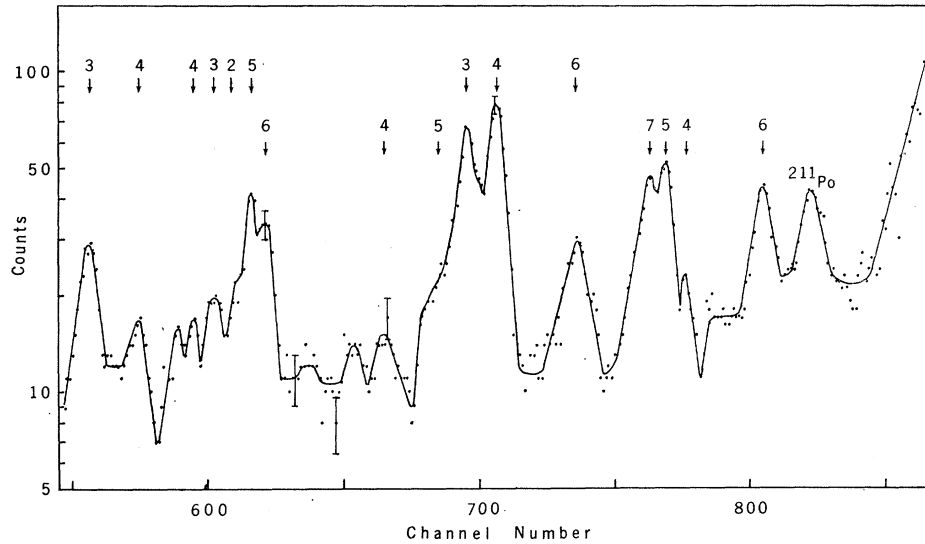


FIG. 2. Low-intensity portion of  $\alpha$  spectrum of  $^{212}\text{At}$  obtained in run A. Lower set of arrows refers to peaks assigned to  $^{212m}\text{At}$ . Upper set of arrows refers to peaks assigned to  $^{212g}\text{At}$ . Numbers give angular momentum ( $J$ ) of states in daughter nucleus  $^{208}\text{Bi}$ .

TABLE III.  $\alpha$  energies and intensities for  $^{212}\text{At}$ .

Initial state ( $J^\pi$ )	Final state ( $J^\pi$ )	Energy <sup>a</sup> (MeV)	Intensity (%)
	5+	7.679±0.001	80.9±0.8
	4+	7.616±0.001	17.0±0.5
	6+	7.170±0.004	0.26±0.06
	4+	7.076±0.005	0.63±0.06
	5+		<0.40
1-	3+	7.045±0.002	0.50±0.08
	7+		<0.10
	5+	6.799±0.002	0.26±0.03
	2+	6.777±0.003	0.04±0.03
	3+	6.754±0.002	0.12±0.03
	4+	6.730±0.005	0.06±0.02
	4+	6.668±0.001	0.05±0.02
	3+	6.612±0.001	0.15±0.01
	6+		<0.02
	5+	7.900±0.001	29.9±0.3
	4+	7.837±0.001	67.3±1.0
	6+	7.391±0.001	0.65±0.07
	4+	7.300±0.004	0.11±0.03
	5+	7.276±0.001	0.53±0.04
9-	3+		<0.40
	7+	7.253±0.002	0.61±0.11
	5+	7.016±0.005	0.26±0.13
	2+		<0.02
	3+		<0.02
	4+	6.954±0.003	0.16±0.10
	4+		<0.10
	3+		<0.03
	6+	6.816±0.003	0.19±0.12

<sup>a</sup> Errors on  $\alpha$  energies do not include an 8-keV systematic uncertainty.

of events but had slightly poorer resolution. The energies and intensities listed in Table III are based on averages of both runs. In Fig. 2, the four most intense peaks at the highest energies are omitted in order to emphasize low-intensity peaks. Because of the low statistics, the data points in Fig. 2 have been smoothed by taking a three-channel running-average.

The energy calibration curves for runs A and B were fitted to the  $^{211}\text{Po}$  peak and the four most intense peaks from  $^{212}\text{At}$ . The energies for these internal standards are listed in Table IV. The assignment of the  $\alpha$  peaks to particular initial and final states given in Table III is based both on the half-life data from Fig. 1 and Table I and on the known energies of the excited states of  $^{208}\text{Bi}$ . The errors given in Table III for the  $\alpha$  energies are rms addition of the error in determining the channel number (0.3 channel=1 keV) and half the energy differences between run A and run B. An additional error of one channel (=3 keV) was included for those peaks which appear as shoulders on other peaks. Note

TABLE IV. Energies of internal standards.

$\alpha$ -particle emitter	$\alpha$ -particle energy
$^{211g}\text{Po}$	7.448±0.001 <sup>a</sup>
$^{212g}\text{At}$	7.616±0.008 <sup>b</sup>
$^{212g}\text{At}$	7.678±0.008 <sup>b</sup>
$^{212m}\text{At}$	7.837±0.008 <sup>b</sup>
$^{212m}\text{At}$	7.899±0.008 <sup>b</sup>

<sup>a</sup> R. J. Walen, V. Nedovessov, and G. Bastin-Schoffier, Nucl. Phys. 35, 232 (1962).

<sup>b</sup> Reference 2.

TABLE V. Levels of  $^{208}\text{Bi}$ .

$J^\pi$	Predicted <sup>a</sup>	$(d, t)$ <sup>b</sup>	$(d, t)$ $(^3\text{He}, d)$ <sup>c</sup>	$^{212g}\text{At}$ <sup>d</sup>	$^{212m}\text{At}$ <sup>d</sup>	$\gamma$ <sup>e</sup>
5+	0.000	0.060	0.000	0.000	0.000	...
4+	0.081	0.063	0.060	0.065	0.064	0.0643
6+	0.529	0.513	0.513	0.519	0.519	0.5103
4+	0.596	0.605	0.603	0.614	0.611	...
5+	0.622	0.634	0.635	...	0.636	...
3+	0.630	0.634	0.635	0.647	...	...
7+	0.664	0.651	0.656	...	0.659	0.6501
5+	0.916	0.890	0.890	0.897	0.901	...
2+	0.920	0.929	0.927	0.919	...	...
3+	0.988	...	0.940	0.943	...	...
4+	0.981	0.963	0.963	0.967	0.964	...
4+	1.060	...	1.040	1.030	...	...
3+	1.046	1.074	1.075	1.087	...	...
6+	1.079	1.098	1.108	...	1.104	...
10-	1.687	...	1.576	...	...	1.5711

<sup>a</sup> Reference 3.<sup>b</sup> Reference 4.<sup>c</sup> Reference 5.<sup>d</sup> Present work.<sup>e</sup> Reference 6.

that a systematic error of 8 keV because of the uncertainty in the calibration curve is not included in the errors listed in Table III.

Before determining the peak intensities, a constant background of 10 counts per channel was subtracted from the data shown in Fig. 2. This background was determined from the flat region of the spectrum below 6.6 MeV and is believed to be due to tailing from the four intense  $\alpha$  peaks. The integration of the areas of the four intense peaks is thought to be accurate to 1%. This error was combined by rms addition with half the differences between the intensities determined in runs A and B to obtain the errors listed for these peaks in Table III. The errors listed for the low-intensity peaks were determined in a similar manner except that integration of the peak areas was assumed to be accurate to 5%.

The  $\alpha$  kinetic energies listed in Table III were corrected for recoil loss to obtain  $Q$  values for  $\alpha$  decay to the various excited states of  $^{208}\text{Bi}$ . The energies of the excited states were obtained by difference from the ground-state transition. These excited-state energies are listed in Table V and are compared with the theoretical and experimental values from published works. The average energy deviation between states populated by both  $^{212g}\text{At}$  isomers is 2 keV which is a measure of the internal consistency of the  $\alpha$  data. The average energy deviation between states measured here and the most recent reaction study<sup>5</sup> is about 6 keV.

Previous reaction studies have been unable to resolve the 3+ and 5+ doublet at about 635 keV. However, the  $\alpha$  decay from  $^{212g}\text{At}(J = 1-)$  preferentially populates the 3+ rather than the 5+ state, and  $^{212m}\text{At}(J^\pi$

$= 9-$ ) preferentially populates the 5+ rather than the 3+. The energy difference between these two states as observed by  $\alpha$  decay is 11 keV with the 3+ state at higher energy than the 5+. This agrees well with the predicted order and with the predicted energy difference of 8 keV.<sup>3</sup>

### III. DISCUSSION

The shell model predicts that odd neutrons and odd protons just beyond the double-closed shells at  $^{208}\text{Pb}$  will occupy  $g_{9/2}$  and  $h_{9/2}$  orbitals, respectively. As discussed by Valli and Hyde<sup>2</sup>, and Torgerson, Gough, and Macfarlane,<sup>11,12</sup> the odd-odd nuclides with 127 neutrons systematically show isomerism. The  $g_{9/2}$  and  $h_{9/2}$  states couple to give 1- and 9- isomers for  $^{210}\text{Bi}$ ,  $^{212}\text{At}$ ,  $^{214}\text{Fr}$ , and  $^{216}\text{Ac}$ . The shell model with a tensor force works well in predicting the order and spacing of levels in  $^{210}\text{Bi}$ .<sup>7</sup> The same tensor force was also used in predicting the excited states of  $^{208}\text{Bi}$ ,<sup>3</sup> and the agreement with experiment is good as was shown in Table V.

The  $^{208}\text{Bi}$  calculations<sup>3</sup> give eigenfunctions for all the states observed in the present work. Hence, it would be possible to use these eigenfunctions to calculate relative reduced widths for the  $\alpha$  transitions from each  $^{212}\text{At}$  isomer using the theories of Mang,<sup>13</sup> Harada,<sup>14</sup> and Rasmussen.<sup>15</sup> The reduced widths when combined with barrier penetration factors could be used to calculate

<sup>11</sup> D. F. Torgerson, R. A. Gough, and R. D. Macfarlane, Phys. Rev. **174**, 1494 (1968).

<sup>12</sup> D. F. Torgerson and R. D. Macfarlane, American Chemical Society National Meeting Paper No. NUCL-45, 1969 (unpublished).

<sup>13</sup> H. J. Mang, Z. Physik **148**, 582 (1957).

<sup>14</sup> K. Harada, Prog. Theoret. Phys. (Kyoto) **26**, 667 (1961).

relative intensities for the possible  $\alpha$  transitions from  $^{212}\text{At}$ . Comparison of the theoretical and experimental intensities could provide information on possible configuration mixing in the  $^{212}\text{At}$  parent or could suggest possible modifications to the  $^{208}\text{Bi}$  wave functions. Detailed theoretical calculations of the relative reduced widths are therefore highly desirable.

<sup>15</sup> J. O. Rasmussen, Nucl. Phys. **44**, 93 (1963).

#### ACKNOWLEDGMENTS

I wish to acknowledge helpful discussions with J. O. Rasmussen concerning the calculation of  $\alpha$  reduced widths. I also wish to thank the cyclotron crew under John Hood for providing good cyclotron beams. The Washington University computing facilities are supported by National Science Foundation Grant No. G-22296.

### Magnetic Moments of Compound States in $\text{Er}^{163}\dagger$

K. H. BECKURTS\* AND G. BRUNHART

*Physics Department, Brookhaven National Laboratory, Upton, New York 11973*

(Received 29 September 1969)

A polarized-neutron transmission method is used to determine the shift of the neutron resonance energies due to the hyperfine interaction of the compound states. Resonances in  $\text{Er}^{167+n}$  at 0.460 and 0.584 eV are investigated. The resonance at 0.584 eV ( $J=I-\frac{1}{2}$ ) shows a strong effect, leading to a very large value of the  $g_J$  factor, while  $g_J$  for the 0.460-eV resonance ( $J=I+\frac{1}{2}$ ) is in the order of  $g_I$  for the  $\text{Er}^{167}$  ground state. The results are compared to some recent predictions based on a statistical model of the compound nucleus. The role of nuclear magnetic interference terms which lead to a strong background transmission effect is discussed.

#### I. INTRODUCTION

RESONANCE capture of slow neutrons by a non-fissile heavy nucleus leads to a highly excited compound state which decays through the emission of a  $\gamma$ -ray cascade with an average lifetime of  $\approx 10^{-14}$  sec. While many efforts have been made in the past to study various properties of these compound states, e.g., their spins and their partial and total widths, to our knowledge no measurements of their magnetic moments have been made so far. The difficulty is that techniques normally used for the determination of magnetic moments of excited states, e.g., the spin precession method or the observation of perturbed angular correlations, cannot be used. Probably the only method, as previously pointed out by Shapiro,<sup>1,2</sup> is direct observation of the shift in the position of the resonance energy due to the interaction between the magnetic moment of the compound state and a very strong magnetic field. Since this shift is expected to be small, measurements with extremely high statistical accuracy, which require a very high neutron intensity, have to be performed.

Using the polarized beam from the high-resolution crystal spectrometer at the Brookhaven high flux beam reactor, we have observed the energy shift due to the

magnetic interaction of the compound state for the neutron resonances in  $\text{Er}^{167}$  at 0.460 eV ( $J=4$ ) and 0.584 eV ( $J=3$ ). The experimental method and the theoretical background are described in Sec. II and the Appendix, while details of the equipment and the experimental procedures are discussed in Secs. III and IV. Experimental results and discussions are given in Secs. V and VI.

#### II. THEORY OF THE MEASUREMENT

Let us consider the interaction between a slow ( $s$ -wave) neutron and a spin-zero nucleus which is in a magnetic field  $H$  parallel to some direction  $z$ . If the interacting neutrons are polarized parallel (or antiparallel) to this  $z$  direction, the resulting compound nucleus will also be polarized parallel (or antiparallel) to the  $z$  direction. If, furthermore,  $E_0$  is the resonant energy of a compound state in the absence of the magnetic field, the energy with the field present becomes

$$E^* = E_0 \mp \Delta E, \quad \Delta E = \mu H \quad (1)$$

where  $\mu$  is the magnetic moment of the compound state and where the  $-$  sign holds for the parallel and the  $+$  sign for the antiparallel orientation of the neutron spin. (The energy is given above the neutron binding energy, and differences between the center-of-mass and the laboratory systems are neglected.) Assuming that the neutrons originate in a region far away from the magnetic field with an energy  $E$ , the total cross section for the interaction of the neutrons and the target nucleus in the neighborhood of a resonance, neglecting the contributions of potential and

<sup>†</sup> Work performed under the auspices of the U.S. Atomic Energy Commission.

\* Permanent address: Institut für Angewandte Kernphysik, Kernforschungszentrum, Karlsruhe, W. Germany.

<sup>1</sup> F. L. Shapiro, in *Proceedings of the Panel on Research Applications of Nuclear Pulsed Systems* (International Atomic Energy Agency, Vienna, 1967), p. 176.

<sup>2</sup> F. L. Shapiro, in *Proceedings of the International Conference on Polarized Targets and Ion Sources, Saclay, France, 1966* (La Documentation Française, Paris, France, 1967), p. 339.